NASA TECHNICAL MEMORANDUM

NASA TM X-67864

NASA TM X-67864

OXIDATION SCREENING AT 1204° C (2200° F) OF CANDIDATE ALLOYS FOR THE SPACE SHUTTLE THERMAL PROTECTION SYSTEM

by W. A. Sanders and C. A. Barrett
Lewis Research Center
Cleveland, Ohio

TECHNICAL PAPER proposed for presentation at
Space Shuttle Materials Conference sponsored by the Society
of Aerospace Material and Process Engineers
Madison, Alabama, October 5-7, 1971

SUMMARY

The oxidation resistance of fifteen alloys was evaluated under some of the environmental conditions that might be encountered by the shuttle thermal protection system. The alloys included nickel-, iron-, and cobalt-base alloys with a sheet thickness of close to 0.38 mm (15 mils). The test specimens were self-resistively heated to 1204° C (2200° F) in 10 torr air for 100 thirty-minute cycles. Specimen weight, thickness and microstructural changes were noted and surface scales were identified by room temperature X-ray diffraction. Based on these observations, the behavior of the alloys was evaluated in terms of metal consumption due to rate of oxide build up, the tendency of the oxide to spall and to vaporize.

The oxidation resistance is the greatest when either Cr_2O_3 or Al_2O_3 formed as the major surface oxide. Spalling occurred when spinel formation accompanied Cr_2O_3 or Al_2O_3. Vaporization of Cr_2O_3 takes place when it is present exclusively, or with a chromite spinel. The presence of an Al_2O_3 layer with the Cr_2O_3 layer, however, inhibits vaporization. The alloy with the best oxidation resistance was TD-NiCrAlY while TD Nickel had the poorest oxidation resistance.

E-6404

OXIDATION SCREENING AT 1204° C (2200° F) OF CANDIDATE ALLOYS FOR THE SPACE SHUTTLE THERMAL PROTECTION SYSTEM

W. A. Sanders and C. A. Barrett
National Aeronautics and Space Administration
Lewis Research Center
Cleveland, Ohio

Abstract

The oxidation resistance of fifteen alloys was evaluated under some of the environmental conditions that might be encountered by the shuttle thermal protection system. The alloys included nickel-, iron-, and cobalt-base wrought alloys. Specimens were self-resistively heated to 1204° C (2200° F) in a 10 torr still air environment for 100 thirty-minute cycles. Specimen weight, thickness and microstructural changes were noted and surface scales were identified by room temperature X-ray diffraction. Based on these observations, the behavior of the alloys was evaluated in terms of overall amount of metal consumption due to oxide formation and relative tendency toward oxide spalling and scale vaporization.

1. INTRODUCTION

Oxidation resistant sheet alloys have been suggested for use as a thermal protection system material (TPS) for the space shuttle. The shuttle thermal protection system (TPS) requires that large surfaces be exposed to 1204° C (2200° F) at low pressures in the 7-20 torr range. It will also be exposed to very high reentry velocities (>Mach 10). Since the shuttle is to be reusable for at least 100 cycles, cyclic exposure is also involved. Basically nonload bearing panels would be used. For this application the candidate classes of materials are: coated refractory metal alloys, compacted ceramic fibers, ablatives and oxidation resistant high temperature alloys such as superalloys and heater alloys (i.e. nickel, iron and cobalt base).(1, 2)

Oxidation resistant high temperature alloys are of particular interest because, hopefully, they might be used uncoated. This would eliminate an added weight and reliability problem. Also, the oxides usually formed on these alloys have a fairly high thermal emittance for efficient reradiation of heat. Generally, there is also a wealth of background experience available in producing and fabricating these alloys. A recently developed alloy, TD NiCr, a thoria dispersioned strengthened Ni - 20 Cr sheet alloy has received particular attention due to its reported excellent oxidation resistance and high temperature strength.(3-7)

Three factors were considered critical in evaluating the relative merits of candidate alloys for oxidation resistance for the shuttle TPS. They are:

(1) The oxidation rate, or how fast the oxide builds up on the surface of the alloy. If the oxide builds up slowly, it is said to be protective and the rate of metal consumption is low.
(2) The vaporization rate, or how fast the scale that forms on the surface sublimes from the surface at temperature. If the oxide vaporizes at an excessive rate, the remaining oxide is too thin to protect the metal and the metal consumption rate is increased.
(3) The spalling rate, or to what extent the scale that forms on the surface cracks and flakes off during each cooling cycle. If the spalling rate is excessive, the effective oxide available for protection is minimal so the metal consumption rate is increased.

The purpose of this investigation was to evaluate 15 candidate high temperature sheet alloys, in terms of these critical factors. This was done by resistively heating the 0.38 mm (15 mils) thick sheet alloy sam-

ples to 1204° C (2200° F) for 100 thirty-minute cycles at an air pressure of 10 torr. The oxidation resistance was evaluated by weight change, appearance, X-ray identification of the scales, and metal thickness change and nature of oxide formed on the alloy based on metallographic examination. The alloys studied were: (1) nickel base - TD Ni, TD NiCr, TD NiCrFe, TD NiCrAlY, DH 245, IN 601, IN 702, Hastelloy X, Tophet 30, and DS NiCr, (2) iron base - Allegheny Ludlum A.1, Hoskins 875, GE 1541 and GE 2541, and (3) cobalt base - HA 188.

2. MATERIALS

The alloys studied are listed in Table I along with their analyzed chemical compositions where available. They consisted of 15 high temperature sheet alloys. Of these, 10 were nickel base and 5 of these nickel base alloys were thoria dispersioned strengthened. These were basically Ni-Cr or Ni-Cr-Al alloys with the exception of TD Ni. DS NiCr is similar to TD NiCr except the alloy is produced by diffusing Cr into a thoria dispersion strengthened nickel. These alloys in general combine good oxidation resistance with comparatively good strength above 1093° C (2000° F).

Four iron base alloys were included based on the Fe - Cr - Al systems which usually have excellent oxidation resistance even approaching 1204° C (2200° F). Their high temperature strength is low, however. Five of the alloys contained a small amount (1 percent or less) of the Group IIIB elements of Y, La, or Ce. These supposedly inhibit oxide spalling.(8)

One cobalt base sheet alloy was also included because of its promising high temperature oxidation and strength properties at 1093° C (2000° F).

Where available, 0.38 mm (15 mil) thick samples were tested in the as-received condition. If the as-received sheet was greater than 0.49 mm (20 mil), the sheet was cold rolled to 0.38 mm and used in the as-rolled condition. The thickness of the alloys varied from 0.27 mm (10.6 mils) to 0.49 mm (19.3 mils).

3. APPARATUS AND PROCEDURE

A schematic of the oxidation test rig in which specimens were cyclically self resistance heated at 10 torr is shown in Figure 1. The cylindrical stainless steel chamber of the test rig is 61 cm (24 in.) high and 25.4 cm (10 in.) in diameter. The water-cooled chamber is split vertically and hinged so that the whole front of the chamber opens. Two horizontal 1.91 cm (0.75 in.) diameter copper electrodes spaced 8.92 cm (3.5 in.) apart enter the tank in the back half way up. The chamber was evacuated by a 425 liter/min mechanical pump through a port in the bottom of the chamber. To maintain the tank at the desired 10 torr test pressure, the mechanical pump worked against two manual variable leak valves in parallel attached to the top of the tank. Each leak valve was open to the atmosphere through a 20-30 micron filter. The leak is offset from the center of the tank and about 40 cm (16 in.) from the mounted sample to minimize any streaming effect of the entering gas. The pressure in the tank was monitored by an absolute diaphragm type 0-50 torr pressure gage. The pressure sensor tubes were arranged so pressures could be read at several locations in the tank.

Prior to test, the 1.27 cm (0.5 in.) x 7.62 cm (3 in.) sheet sample was ultrasonically degreased and cleaned. It was then weighed to the nearest 0.1 mg and its thickness measured at the center with a micrometer to the nearest 0.001 mm (0.04 mils). To prepare for a test, the sample was fixed in place against the copper electrodes with mounting brackets. The specimen was centered with the long axis horizontal and parallel to the bottom of the chamber. The chamber door was then closed and the chamber evacuated. The manual leaks were always kept open to protect the pressure gage and held to near the same settings. Within a few minutes the chamber pressure stabilized to 10 torr. Power was then supplied to the sample and the sample temperature measured by an optical pyrometer. The optical pyrometer was calibrated against an NBS standard lamp and temperature corrections were made for the quartz window and an assumed sample emittance of 0.9. This is the emittance value for oxidized nichrome.(9) Although other oxides in addition to, or instead, Cr_2O_3 were present on some of the materials tested, it was assumed that their emittance was close to $\epsilon = 0.9$. For samples where the emittance was less than $\epsilon = 0.9$, the actual test temperature exceeded 1204° C (2200° F). For example, if the oxidized sample has an emittance as low as $\epsilon = 0.7$ then its's temperature would be close to 25° C hotter than a sample of emittance equal to 0.9.

It usually took 2-3 minutes to bring the sample to temperature, and at this point automatic timers were activated. A 30 minute heating cycle and a 6 minute cooling cycle were used. At the end of 30 minutes the power was cut off instantaneously and the sample cooled in a few seconds to room temperature. When the heating cycle was activated, the previous power settings were again instantaneously applied to the sample and the sample rapidly heated to temperature. Generally, depending on the alloy and its thickness, around 2 to 3 volts were used with currents of 50 to 200 amps. After the initial cycle the temperature held constant with an occasional adjustment. The pressure also held nearly constant at 10 torr. Both, on the average, were held close to 1 percent of their desired value by adjusting their controls once a day. Since the sample was constrained at both electrodes, it bowed upon heating since it was not free to expand.

The temperature distribution horizontally along the face of the sample is shown schematically in Figure 2.

After the test was completed (100 30-minute cycles), the sample was removed and its appearance noted. The sample was then reweighed to the nearest 0.1 mg. The bowed sample was then straightened without disturbing the surface so that a surface X-ray diffraction pattern could be obtained to determine the surface oxide(s) present. A GE-XRD-6 diffraction unit was used with Cu radiation at 40 KV and 40 ma with a monochromator. The sample was then mounted in epoxy and sectioned as indicated in Figure 2. Metallographic examination was performed to determine both the thickness change and the nature of the oxide and the alloy. The thickness change was determined from the difference between initial thickness near the center of the sample measured with a mm micrometer and the metal thickness measured after test metallographically under a microscope. The sample was mounted and sectioned so that the thickness was measured at point A in Figure 2. Thickness was taken as the average of 5 measurements at different locations near point A. This thickness measurement was from oxide surface layer-metal interface to oxide surface layer-metal interface and did not include internal oxidation effects or grain boundary oxide penetration.

4. RESULTS

The principal types of observations made in this study were appearance of the sample after test, weight change, nature of the retained oxide on the sample as determined by X-ray diffraction, thickness change, and microstructure. These are discussed in the following sections.

4.1 APPEARANCE

A brief description of each sample after test is given in Table II. It should be noted that all samples bowed upon heating during test and remained bent to a lesser degree upon cooling. After test, the sample midpoint was usually displaced about 0.6 cm (1/4 in.) from the original vertical plane of the specimen (see Fig. 3). Usually the scale formed on a sample appeared quite uniform to within about 0.9 cm (3/8 in.) of each end. Also indicated in Table II was any tendency for the scale on the samples to spall or flake off. Spalling was considered to be moderate if it was local in nature or occurred just on the ends. Heavy spalling was classified as being general over the whole oxidized part of the specimen. Any other unusual feature such as the specimen being badly warped (i.e. puckered) or distorted is also noted.

Most of the samples had uniform light thin oxides similar in shading to Figure 3. The samples IN 601, Hastelloy X, and HA 188 had dark puckered scales and sample distortion. Other alloys showing distortion were IN 702, DH 245, Alleg Lud. A.1, Hoskins 875 and HA 188. Light spalling was detected for Tophet 30, IN 702, and DH 245. Heavy spalling was found on IN 601 and Hastelloy X. Hoskins 875 was the only sample that cracked when straightened after test for X-ray analysis.

4.2. WEIGHT CHANGE

The change in weight of a test sample after test is shown graphically in Figure 4 for each alloy. Also plotted on the left hand scale is weight change per unit area after 50 hours. Based on appearance and on temperature distribution, an approximate area of 16.0 cm^2 was used in order to provide a rough comparison with other oxidation data. All samples showed observable oxidation even after the first 30-minute cycle. A positive weight change is taken to imply that formation of oxide is the dominant process occurring. Conversely, a weight loss implies loss of scale by vaporization and/or spalling.

The weight changes were positive for 8 alloys ranging from a high of approximately 90 mg for TD Ni to just barely positive for IN 601. The alloys that lost weight showed a negative weight change close to 10.0 mg except for Hastelloy X which lost about 100 mg.

4.3. NATURE OF THE RETAINED SURFACE OXIDE

A summary of these results is listed in Table III. In all cases except for Allegheny Ludlum A.1, the underlying solid solution alloy was detected under the surface scale. This implies the entire thickness of the oxide was analyzed. The oxides themselves were identified as indicated in the table. The intensities of the observed oxide(s) are also noted. These are relative ratings of the peaks in a given scan. When more than one oxide is present, the relative intensities may either be an indication of the relative amounts present or how the oxides were layered on the surface or a combination of both.

In addition to Cr_2O_3, Al_2O_3, and NiO, oxides having the spinel structure were also identified as scale components. Spinels are cubic oxides which in their most simple form are $MeO\text{-}Ma_2O_3$, where Me is the base metal, here either Ni, Fe or Co, and Ma is either Cr or Al. Some of the more common spinels are listed at the bottom of Table III along with their lattice parameters, a_o. In general, a lattice parameter of 8.30 angstroms (Å) or higher implies a chromite spinel while that close to 8.10 Å implies an aluminate spinel.10) Solutions of aluminate and chromite would have intermediate lattice parameters depending on the amount of each.

Cr_2O_3 was found exclusively on the surface of TD NiCr, TD NiCrFe and DS NiCr, and was found as a major oxide along with a chromite spinel on Tophet 30, IN 601,

Hastelloy X, HA 188 and Allegheny Ludlum A.1. Al_2O_3 was found exclusively on TD NiCrAlY and Hoskins 875 and with aluminate spinels on DH 245 and IN 702. Al_2O_3 and Cr_2O_3 were found together on GE 1541 and GE 2541 along with chromite spinels. Only NiO formed on TD Ni. ThO_2 was detected for all the thoria strengthened alloys except TD Ni.

4.4. THICKNESS CHANGE

The metal loss per side of an oxidized sample is shown graphically in Figure 5 for each of the 15 test alloys. The validity of this measurement is based on the assumption that the thickness of the metal will decrease as the metal is converted to oxide. As more oxide is formed, regardless of whether it stays on the alloy, spalls or vaporizes, the metal will be consumed and the alloy will grow thinner, assuming sample creep is not a factor. For the purpose of rating the alloys, the thickness change after test was ranked as small (0.0 to 0.010 mm), moderate (0.010 to 0.020 mm) or high (greater than 0.020 mm) (see Fig. 5).

Based on this ranking, the alloys, TD NiCr, TD NiCrAlY, TD NiCrFe, DS NiCr, HA 188, GE 2541, and GE 1541 have small thickness changes; Tophet 30, DH 245, IN 702, and Hoskins 875 fall into the moderate thickness change region; TD Ni, IN 601, Hastelloy X and Allegheny Ludlum A.1 show a large thickness change.

4.5. MICROSTRUCTURE

Microstructural examination was made on each test specimen across the thickness of the sample close to its midpoint. (See Fig. 2, point A.) The samples were examined both in the unetched and etched conditions. In all cases an electrolytic etch was used consisting of 100 ml H_2O, 2 gm chromic acid and 10 ml H_2SO_4. Examination in the unetched condition (in which the thickness determinations were also made) was used to note the features of the specimen primarily concerned with oxidation of the sample, while examination in the etched condition revealed structural features of the alloys. Figures 6 to 20 show all the samples individually, each at a magnification of 200 and unetched to include all of the cross section, and at a magnification of 500 in the etched condition to show the oxide/metal interface.

From an oxidation standpoint the characteristics of the alloys can be grouped as follows:

(1) Uniform tight adherent scale, no significant grain boundary oxidation.
    (a) TD NiCr, TD NiCrFe, DS NiCr (very thin scales on the order of 0.0015 mm (0.06 mils)
    (b) TD NiCrAlY (thin scales each close to 0.006 mm (0.24 mils).
    (c) TD Ni (thick scale 0.07 mm (2.8 mils)).
(2) Uniform tight adherent scale, significant grain boundary oxidation - GE 2541, GE 1541 (thin scales each close to 0.006 mm (0.24 mils)).
(3) Uniform tight adherent scale, occasional cracks due to local spalling. No significant grain boundary or internal oxidation - DH 245, HOS 875 (thin scales each close to 0.006 mm (0.24 mils)).
(4) Simple to complex scale(s) (>0.006 mm (0.24 mil)), showing various degrees of spalling, and grain boundary oxidation - Tophet 30, IN 601, HAS X, IN 702, HA 188, and Allegheny Ludlum A.1.

The alloys falling into category (4) are difficult to differentiate from each other, but they definitely appear more complex in their oxidation behavior than the first three categories. Group (4) alloys apparently oxidize more severely than the other alloys except for TD Ni.

Grain boundary oxidation occurs in GE 1541, GE 2541, IN 702, IN 601 and Allegheny Ludlum A.1.

5. DISCUSSION

In the oxidation of metals and alloys three basic processes should be considered. First is the formation of the scale on the metal surface due to parabolic (i.e. diffusion controlled) oxidation. The resulting weight gain curves at a given temperature increase parabolically with time. In terms of thickness change the metal decreases and the oxide increases parabolically with time.

The second process to consider is vaporization of the scale. If, as the oxide forms it also tends to vaporize, it will leave the surface at a linear rate. In terms of overall measured weight change, as a function of time, the curve will in most cases pass through a maximum after an initial parabolic rate. The curve will then decrease as the vaporization becomes dominant, eventually passing into a negative weight change region where the weight loss of the vaporized metal oxide exceeds the total weight of the oxygen reacted with the metal. Under this condition the scale will stay relatively thin and at nearly a constant thickness, while the metal will be consumed at nearly a constant rate. The higher the vaporization rate relative to the diffusion controlled oxidation rate, the thinner the oxide will become and the faster the curve will approach negative values. This in turn will increase the metal consumption rate since the diffusion paths for the reacting species are shorter.[6,7,11,12]

The third important process in metal oxidation is the

tendency for the oxide to spall or flake off due to scale cracking usually when the sample is cooled from elevated temperature. This tendency is based on many factors such as cooling rate, geometry of the sample, thickness of scale formed, etc. It is due to the difference in thermal expansion, strength and plasticity of the phases present in the scale and the underlying metal. Spalling is difficult to define and measure precisely since it is usually a function of how the test was run. Usually a test cycle is chosen which reasonably simulates the actual service conditions. The spalling is detected either by macroscopic observation (actually by seeing the scale flake off, or from evidence that it has) and/or microscopic observation of the scale which indicates that it is nonadherent, nonuniform and cracked or fissured.

If a cyclic oxidation test is run and a weight change curve is generated, it is parabolic (in the absence of vaporization) for only the first cycle if spalling occurs on cooling. Then it can, in the most extreme case, lose all of the oxide formed at temperature when it cools. The oxide reforms when the sample is reheated but with the same high initial rate as before. This rapidly consumes the metal with each cycle. If, on the other hand, spalling is only partial or intermittent, then the curve deviates less from the ideal parabolic weight gain curve.

The most complex case is when both vaporization of the oxide is taking place while the metal is oxidizing at temperature, and spalling is taking place as the sample is cooled. Here, the resulting weight change curves can be very complex depending on the relative contribution of the three basic processes. Spalling effects, particularly if severe, tend to mask vaporization effects. In this case, vaporization is assumed if a similar oxide appears to vaporize on other alloys where spalling is not detected (e.g. Cr_2O_3 vaporizes on TD NiCr, therefore it is assumed it does also on Tophet 30).

All three of the basic oxidation processes contribute to the overall consumption rate of the alloy. Oxide vaporization which is not necessarily severe in slowly moving air at 10 torr and 1204° C (2200° F) could be magnified significantly in high velocity gas flows. Indeed accelerated attack due to scale vaporization has been observed in high gas velocity tests.(13-16)

Using the test results (appearance, weight and thickness change, X-ray diffraction of the retained oxides and microstructure), the alloys tested were rated in terms of the three basic processes. It was the nature of these tests that instead of an oxidation weight change curve being generated as a function of time, only one 50 hour data point is available. Therefore, if no spalling is detectable (either from the sample appearance or from the microstructure) and the weight change after the test is negative, it can be inferred that oxide vaporization took place (i.e. that the weight of the oxide lost by vaporization exceeds the weight of the oxygen reacted). This, however, **does not** mean that vaporization did not occur if the weight change is positive.

The scaling rate is classed as "high" or "low" in the absence of oxide vaporization and spalling if the thickness change of the alloy falls in the high or small Δt portions of Figure 5.

Spalling of the oxide is classified as either "moderate" or "severe" if observed and the thickness change in most cases is in the moderate or high portion of Figure 5.

Based on these rating criteria the alloys can be classed as follows:

I. High scaling rate, no dominant vaporization or detectable spalling. TD Ni (large change in weight, large change in thickness, uniform thick, adherent scale with no cracks. NiO only oxide formed).

II. Low scaling rate, no dominant vaporization or detectable spalling.
   - (a) TD NiCrAlY (small change in weight, small change in thickness, uniform thin, adherent scale with no cracks. Al_2O_3 only oxide formed.)
   - (b) GE 1541, GE 2541 (same as II(a), but significant grain boundary oxidation also present. Al_2O_3 major oxide found along with some Cr_2O_3 and an iron chromite spinel).

III. Low scaling rate, dominant vaporization, no detectable spalling. TD NiCr, TD NiCrFe, and DS NiCr.
   (Negative change in weight, small change in thickness, uniform, very thin adherent scale with no cracks. Cr_2O_3 major oxide found.)

IV. Low scaling rate, no dominant vaporization, detectable spalling. DH 245, IN 702, and HOS 875.
   (Small positive or negative weight change, moderate thickness change, macro appearance - apparent moderate spall, except for HOS 875. Micro appearance - intermittent, nonadherent. Al_2O_3 major oxide formed with an aluminate spinel also found on IN 702 and HOS 875. Spalling on HOS 875 appeared due to specimen creep. IN 702 also showed finger-like grain boundary oxidation.)

V. Low scaling rate, dominant vaporization and detectable spalling.
   - (a) HA 188 (negative weight change, small thickness change, macro appearance - apparent moderate spall, micro appearance - thin nonuniform oxide, intermittent nonadherent Cr_2O_3 major oxide with a cobalt chromite spinel).

(b) Tophet 30 (negative weight change, moderate thickness change, macro appearance - apparent moderate spall, micro appearance - thin nonuniform oxide, intermittent nonadherent. Cr_2O_3 major oxide formed with a trace of a nickel chromite spinel).

(c) Hastelloy X (large negative weight change, high thickness change, macro appearance - apparent heavy spall and severe sample distortion. Micro appearance - fissured scale with intermittent nonadherence. Cr_2O_3 and a nickel chromite spinel major oxides).

VI. High scaling rate, dominant vaporization and detectable spalling. IN 602 and Allegheny Ludlum A.1

(Positive weight change due to severe grain boundary oxidation weight gain apparently overrides severe weight loss due to spalling. Macro appearance - apparent heavy spall and severe sample distortion, micro appearance - irregular fissured scale with intermittent nonadherence. Severe grain boundary oxidation. Mostly Cr_2O_3 and chromite spinel major oxides).

From the preceding oxidation ratings based on the test results, the observations can be made:

1. If either Al_2O_3 and/or Cr_2O_3 were formed on the alloy, the scaling rate was low (i.e. small thickness change) implying low diffusion rates in the oxide. If NiO was formed, such as on TD Ni, the oxidation rate was high giving a large metal thickness change. This agrees with the diffusion rate data for cation diffusion which is higher in NiO than in Cr_2O_3 or Al_2O_3. (D_{Ni} in NiO is at least 10 times greater than D_{Cr} in Cr_2O_3 or D_{Al} in Al_2O_3 at 1204° C (2200° F).[17-19]
2. In the alloys where Cr_2O_3 was the primary oxide formed with no spinel or Al_2O_3 present, oxide vaporization dominated the implied oxidation weight change curve at 50 hours (TD NiCr, TD Ni CrFe and DS NiCr). Where a spinel was present vaporization was not inhibited (HA 188 and Tophet 30). If Al_2O_3 were present, however, Cr_2O_3 volatility was inhibited (GE 1541 and GE 2541).
3. If a spinel were present with either Al_2O_3 or Cr_2O_3 the scale(s) tended to spall. Four of the alloys that formed spinels also contained a small amount of the Group III elements Y, La, or Ce which are added in order to inhibit spalling.[8] It apparently helped in only two cases, GE-1541 and GE-2541. In these two cases the X-ray intensities for the spinel were quite weak. Allegheny Ludlum A.1 showed severe spalling and HA-188 moderate spalling.
4. Severe grain boundary oxidation was found in five of the alloys GE 1541, GE 2541, IN 601, Allegheny Ludlum A.1 and IN 702.
5. TD NiCrAlY was the only alloy studied which indicated a low oxidation rate, no detectable oxide spalling or significant vaporization, no apparent grain boundary oxidation, or sample puckering.

6. SUMMARY OF RESULTS

Fifteen high temperature sheet alloys were exposed for 100 thirty-minute cycles at 1204° C (2200° F) at an air pressure of 10 torr in a still air environment. The alloys were rated in terms of their oxidation scaling rate, tendency for the scale to spall due to cyclic oxidation and tendency for the oxide to vaporize. The results may be summarized as follows:

1. The oxidation scaling rate (i.e., diffusion controlled oxidation) is low for all alloys which form either Al_2O_3 and/or Cr_2O_3. This included all of the alloys tested in this study except TD Ni which oxidized to form only NiO on the surface. The NiO formed accounted for the high oxidation rate.
2. Alloys which formed either aluminate or chromite spinels with the Al_2O_3 or Cr_2O_3 showed moderate (DH 245, IN 702, HA 188 and Tophet 30) to severe (IN 601, Hastelloy X and Allegheny Ludlum A.1) spalling. The two other spinel forming alloys, GE 1541 and GE 2541 did not appear to spall. These latter two contained close to 1 w/o of the rare earth Y, however. HOS 875, which formed Al_2O_3 exclusively, spalled due to creep of the alloy.
3. All of the alloys which formed Cr_2O_3 exclusively on the surface (TD NiCr, TD NiCrFe and DS NiCr), indicated a significant degree of oxide vaporization. The presence of a chromite spinel did not appear to inhibit oxide volatility (HA 188, Tophet 30, IN 601, Hastelloy X and Allegheny Ludlum A.1). However, the presence of Al_2O_3 did appear to inhibit Cr_2O_3 vaporization (GE 1541 and GE 2541).
4. Five of the alloys showed pronounced grain boundary oxidation which would tend to limit their load bearing thickness. They were GE 1541, GE 2541, IN 702, Allegheny Ludlum A.1 and IN 601.

7. CONCLUDING REMARKS

Based on this investigation certain guidelines can be inferred for choosing an alloy for the shuttle TPS. Most promising would be a nickel base alloy with a minimum of 3.0 w/o Al and 16.0 w/o Cr. This would favor the formation of Al_2O_3 and/or its spinel (e.g., TD NiCrAlY and IN 702). This would minimize oxide vaporization and provide an alloy with a low oxidation rate. It would

still be a fabricable sheet alloy; however, the low emittance of Al_2O_3 scales would, of course, be of concern for the shuttle application. Therefore, any development effort on Al_2O_3 forming alloys should include efforts to increase emittance. From an oxidation viewpoint both TD NiCrAlY compositions and modifications of IN 702 would appear promising for TPS applications. IN 702 would require modifications to eliminate grain boundary oxidation attack as well as to minimize spalling.

In addition to giving the comparative behavior of alloys in terms of the severity of oxidation and spalling tendencies, some inferences can also be made from this investigation relevant to the tendency of protective scales to be lost by vaporization. The protective ability of Cr_2O_3 is degraded by evaporative loss of the scale. It has been shown that the high velocities associated with the shuttle reentry profile would tend to intensify this loss and make the problem more severe.(16) Thus, gas velocity is an important test parameter not included in this preliminary study that should be included in any critical evaluation to fully describe chromium bearing alloys for shuttle application.

8. REFERENCES

1. Colwell, J. E.; and Kamber, K. T.: Materials and Structures Technology for a Space Transportation System. Paper 70-272, AIAA, Feb. 1970.
2. Bauer, Paul E.; and Kummer, Donald L.: A Survey of Reusable Metallic and Nonmetallic Thermal Protection Materials for Space Shuttle Applications. Paper 70-273, AIAA, Feb. 1970.
3. Anon.: TD Nickel-Chromium. Tech. Note, Defense Metals Information Center, Battelle Memorial Inst., Nov. 2, 1967.
4. Douglas, D. L.; and Armijo, J. S.: Improved Oxidation Resistance of Nickel and Cobalt Base Superalloys. Stanford Research Inst. (NASA CR-91895), Dec. 21, 1967.
5. Rhee, S. K.; and Spencer, A. R.: Oxidation of Common High Temperature Alloys. Metallurg. Trans., vol. 1, no. 7, July 1970, pp. 2021-2022.
6. Giggins, C. S.; and Pettit, F. S.: The Oxidation of TD NiC (Ni-20Cr-2 vol pct ThO_2) Between 900° and 1200° C. Metallurg. Trans., vol. 2, no. 4, Apr. 1971, pp. 1071-1078.
7. Lowell, Carl E.; Deadmore, Daniel L.; Grisaffe, Salvatore J.; and Drell, Isadore L.: Oxidation of Ni-20Cr-$2ThO_2$ and Ni-30Cr-1.5Si at 800°, 1000°, and 1200° C. NASA TN D-6290, 1971.
8. Goward, G. W.: Current Research on the Surface Protection of Superalloys for Gas Turbine Engines. J. Metals, vol. 22, no. 10, Oct. 1970, pp. 31-39.
9. Wood, W. D.; Deem, H. W.; and Lucks, C. F.: Thermal Radiative Properties of Selected Materials. DMIC Rep. 177, vol. 1, Battelle Memorial Inst., Nov. 15, 1962.
10. Joint Committee on Powder Diffraction Standards: Powder Diffraction File, Set 20. ASTM, 1970.
11. Tedmon, C. S., Jr.: The Effect of Oxide Volatilezation on the Oxidation Kinetics of Cr and Fe-Cr Alloys. J. Electrochem. Soc., vol. 113, no. 8, Aug. 1966, pp. 766-768.
12. Lewis, H.: The Kinetics of the Oxidation Process in Nickel-Chromium-Base Alloys. Metallurgia, vol. 83, no. 495, Jan. 1971, pp. 3-8.
13. Probst, Hubert B.: Effect of Environment on Erosion-Corrosion Processes. Aerospace Structural Materials. NASA SP-227, 1970, pp. 279-293.
14. Sanders, W. A.; and Probst, H. B.: Hot Corrosion of TD Nickel and TD Nickel Chromium in a High Velocity Gas Stream. Presented at the Naval Tenth National Conference on Environmental Effects of Aircraft and Propulsion Systems, Trenton, N. J., May 18-20, 1971.
15. Johnston, James R.; and Ashbrook, Richard L.: Oxidation and Thermal Fatigue Cracking of Nickel- and Cobalt-Base Alloys in a High Velocity Gas Stream. NASA TN D-5376, 1969.
16. Centolanzi, Frank J.: Hypervelocity Oxidation Tests of Thoria Dispersed Nickel-Chromium Alloys. NASA TM X-62015, 1971.
17. Kubaschewski, Oswald; and Hopkins, B. E.: Oxidation of Metals and Alloys. Second ed., Academic Press, 1962.
18. Hagel, W. C.; and Seybolt, A. U.: Cation Diffusion in Cr_2O_3. J. Electrochem. Soc., vol. 108, no. 12, Dec. 1961, pp. 1146-1152.
19. Kofstad, Per: High-Temperature Oxidation of Metals. John Wiley & Sons, Inc., 1966.

TABLE I. - SHEET ALLOY TEST SPECIMENS - CHEMICAL ANALYSIS, STARTING THICKNESS AND TEST CONDITION

Alloy	Composition, weight percent								Starting thickness mm (mils)	Test condition
	Ni	Co	Fe	Cr	Al	Si	ThO_2	Other		
TD Nickel	Bal.	0.01	0.01	0.01			2.4	0.003C, .001S	0.49 (19.3)	As received
TD NiCr	Bal.			19.35			2.31	.0076C, .0030S	.49 (19.3)	As received
TD NiCrFe	Bal.		18.14	18.79			2.5	.0205C, .005S	.37 (14.6)	From 0.042"
TD NiCrAlY	Bal.			15.56	4.61		1.56	.25Y	.27 (10.6)	As received
DS NiCr	Bal.	.002	.07	20.8			1.9	.006Cu, .1Mn, .008S, .006C, excess O_2 <100 ppm	.29 (11.4)	
Tophet 30	Bal.	.001	.15	29.63	.3	1.43		.028C, .01Mn	.35 (13.8)	From 0.100"
IN 601	Bal.		13.41	23.05	1.38	.48		.27Mn, .04C	.38 (15.0)	From 0.061"
IN 702	Bal.		.50	15.44	3.08	.22		.99Ti, .04Mn, .04C	.38 (15.0)	From 0.094"
Hastelloy X	Bal.	2.16	18.87	21.31		.33		.07C, .62W, 9.02Mo .018P, .003S, .71Mn	.42 (16.5)	As received
DH-245	Bal.	.03	.7	19.54	3.51	1.22		.4Mn, .034C	.41 (16.1)	From 0.100"
GE-1541	0.25		Bal.	14.5	4.52	.10		.74Y, .002C	.39 (15.4)	As received
GE-2541	.11		Bal.	24.55	3.83	.15		1.23Y, .037C	.34 (13.4)	From 0.100"
Allegheny Lud. A.1[a]	20		Bal.	20	2	.5		.5Mn, .1Ce	.49 (19.3)	As received
Hoskins 875			Bal.	21.44	5.25	.66		.05C, .17Mn	.41 (16.1)	From 0.100"
HA-188	22.84	Bal.	1.69	21.58		.42		.01La, .008P, .005S .61Mn, .11C, 14.04W	.37 (14.6)	From 0.063"

[a] Vendor's nominal.

TABLE II. - DESCRIPTION OF SAMPLES AFTER TEST

Alloys	Description
TD Ni	Uniform dark gray oxide. Greenish tint towards ends. No discernable oxide spalling.
TD NiCr	Uniform thin blue-gray scale. Light blue-gray at ends. No discernable oxide spalling.
TD NiCrFe	Uniform thin blue-gray scale. Light gray at ends. No discernable oxide spalling.
TD NiCrAlY	Uniform thin silver-gray scale. A few greenish oxide patches. Light gray at ends. No discernable oxide spalling.
DS NiCr	Uniform thin blue-gray scale. Green at edges. Light gray at ends. No discernable oxide spalling.
Tophet 30	Uniform dark blue-green scale. Lighter green towards ends. Moderate spalling especially near edges.
IN 601	Black puckered scale. Grayer towards the ends. Apparent heavy spall. Sample distorted.
IN 702	Uniform bright aqua-blue scale with copperish bare spot in center. Gray at ends. Moderate spall and sample distorted.
Hastelloy X	Dark black puckered scale. Gray-black at ends. Apparent heavy spalling and sample distorted.
DH 245	Light gray-green scale with small dark spots. Darker gray-green towards ends. Apparent moderate spall. Sample slightly distorted.
GE 1541	Uniform thin light gray scale. Lighter gray towards ends. No discernable oxide spalling.
GE 2541	Uniform thin silver-gray scale. Same, only lighter, towards ends. No discernable oxide spalling.
Alleg. Lud. A.1	Uniform sooty black scale. Lighter black at ends. Heavy spall and sample slightly distorted.
Hoskins 875	Uniform thin silver gray scale. Light gray at ends. No discernable oxide spalling. Sample cracked when flattened. Sample slightly distorted.
HA 188	Dark purple-green puckered scale. Moderate oxide spalling. Sample distorted.

TABLE III. - PHASES DETERMINED BY X-RAY DIFFRACTION ON ALLOYS CYCLICALLY EXPOSED AT 1204° C (2200° F), 10 TORR AIR PRESSURE, FOR 50 HOURS. TEST CYCLE: 30 MINUTES AT 1204° C (2200° F), 6 MINUTES STILL AIR COOL.

Alloy	-*Adhering surface phases determined by X-ray diffraction-					
	Cr_2O_3	Al_2O_3	NiO	**Spinel a_o in angstroms	ThO_2	Ni-, Co-, or Fe-solid solution
TD NiCr	S				W (from alloy)	P
TD NiCrAlY		S			W (from alloy)	P
TD NiCrFe	S				M (from alloy)	P
DS NiCr	S				M (from alloy)	P
TD Ni			S			P
Tophet 30	S			$a_o \sim 8.35$ VW		P
IN 601	S			$a_o \sim 8.34$ W		P
Hastelloy X	S			$a_o \sim 8.40$ S		P
DH 245		S		$a_o \sim 8.14$ M		P
IN 702		S		$a_o \sim 8.10$ S		P
HA 188	S			$a_o \sim 8.35$ S		P
2541	W	S		$a_o \sim 8.40$ W		P
Hoskins 875		S				P
Allegheny ludlum A1	S			$a_o \sim 8.38$ S		--
1541	M	S		$a_o \sim 8.42$ W		P

*S - Strong, M - Medium, W - Weak, VW - Very Weak, P - Present.

**Lattice parameters in angstrom units for spinels:

$NiAl_2O_4$	8.05 Angstroms
$NiCr_2O_4$	8.32 Angstroms
$CoCr_2O_4$	8.32 Angstroms
$FeCr_2O_4$	8.35 Angstroms

9. BIOGRAPHY

William A. Sanders received his BS in Metallurgical Engineering from the Case Institute of Technology. He has been associated with the Lewis Research Center of the National Aeronautics and Space Administration as a materials research engineer for 15 years. He is presently involved in the evaluation of nickel- and cobalt-base superalloys and non-metallic materials for advanced turbine engine applications. His previous work has involved studies of the compatibility of refractory metals and compounds, and the fabrication and mechanical properties of refractory compounds.

Charles A. Barrett received his BS and MS in metallurgy from Case Institute of Technology and MS in statistics from Western Reserve University. Since joining NASA's Lewis Research Center in 1956 he has worked in the area of high temperature alloy oxidation, refractory metals, statistical design of experiments and liquid metal corrosion. He is currently involved in high temperature oxidation studies for advanced turbine engine and space shuttle applications.

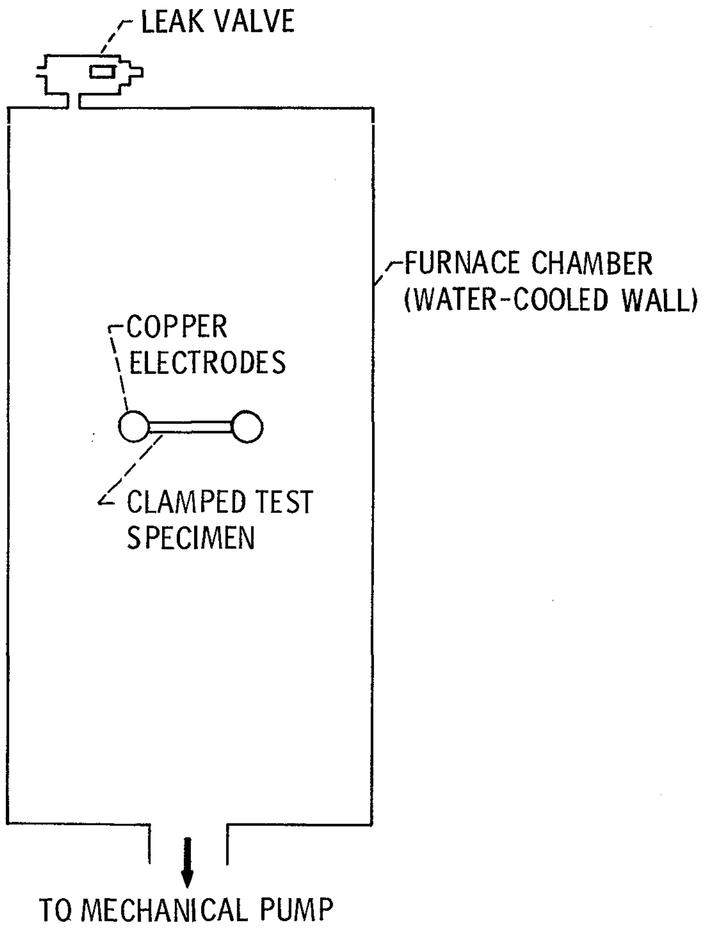

Figure 1. - Schematic of apparatus for reduced air pressure oxidation of self-resistance heated test materials.

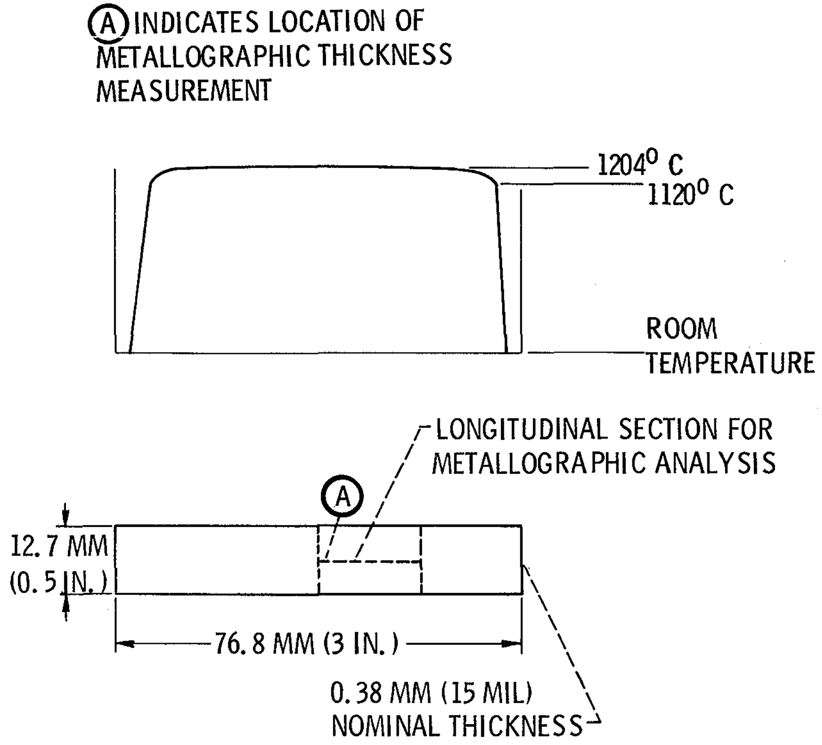

Figure 2. - Sheet specimen for reduced air pressure oxidation test showing sectioning for metallographic analysis. Immediately above is a typical schematic temperature gradient.

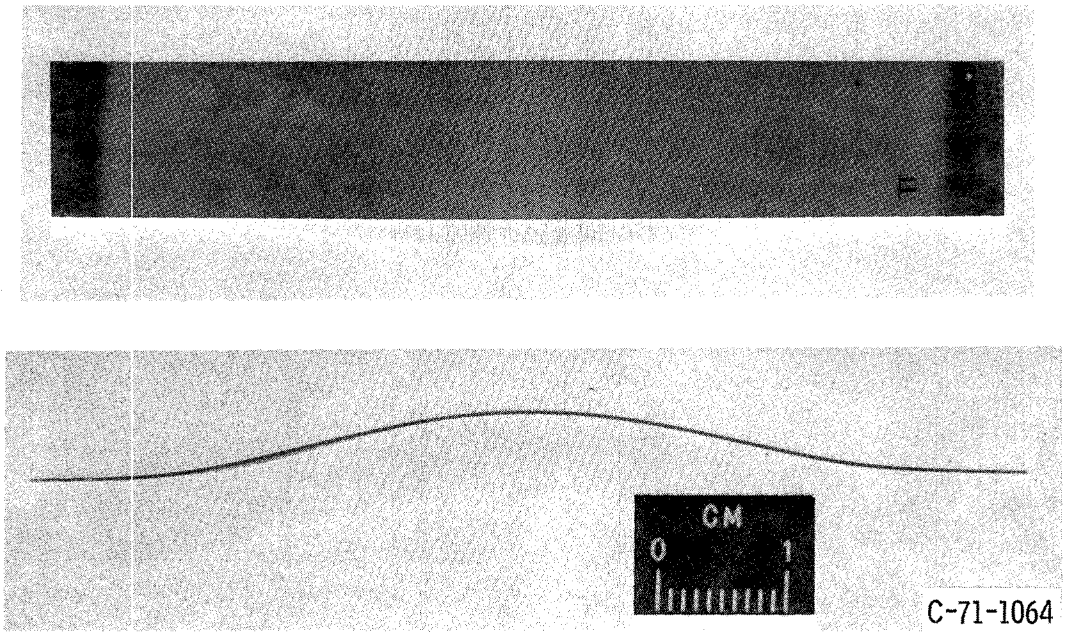

Figure 3. - Typical post-test oxidation sample, TD NiCr, 2200° F, 10 torr. Top-front view showing thin oxide scale, bottom-side view showing bowed sample.

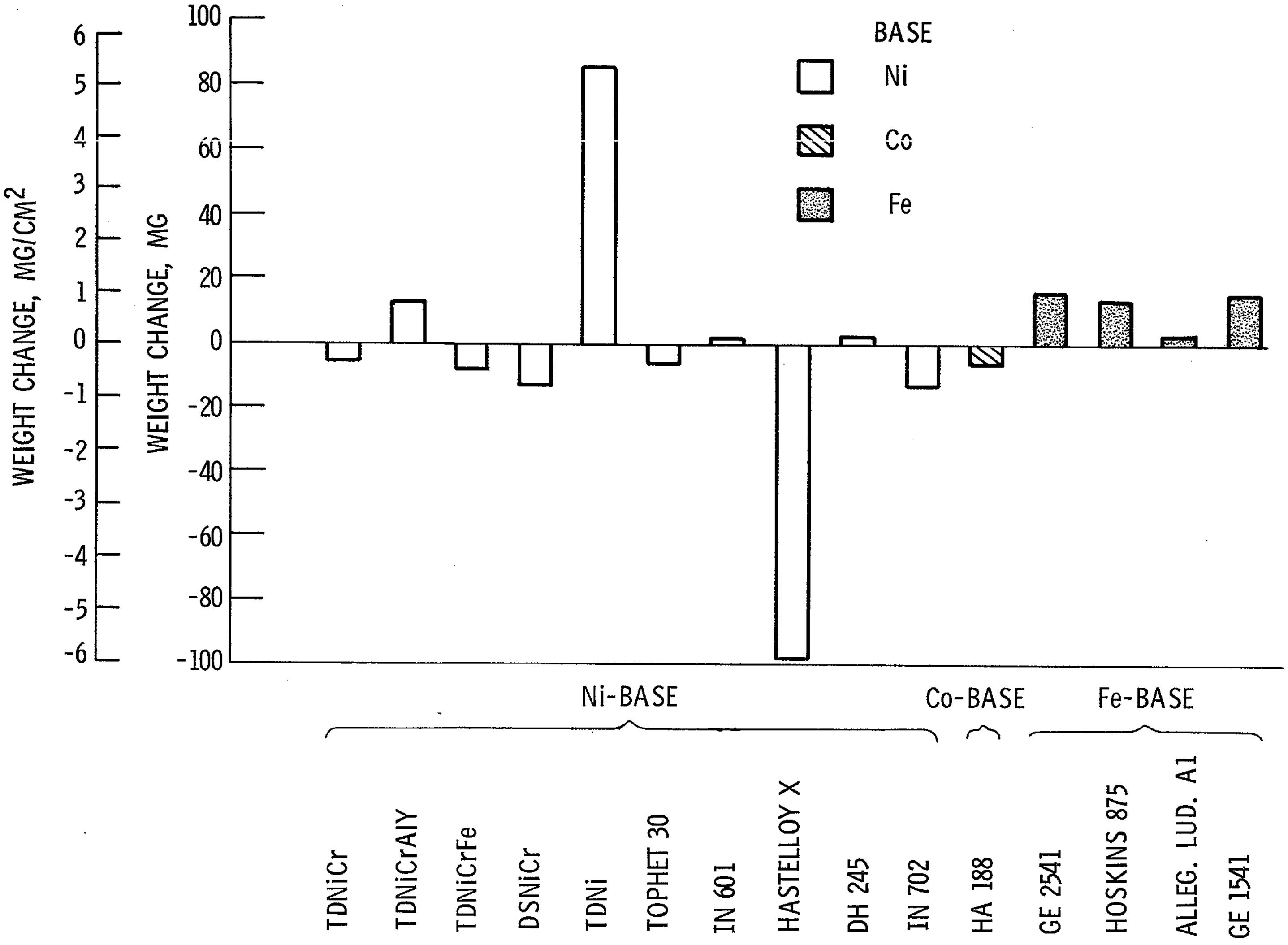

Figure 4. - Weight change for materials cyclically exposed at 1204° C (2200° F), 10 torr air pressure, for 50 hours. Test cycle: 30 minutes at 1204° C (2200 ° F), 6 minute cool.

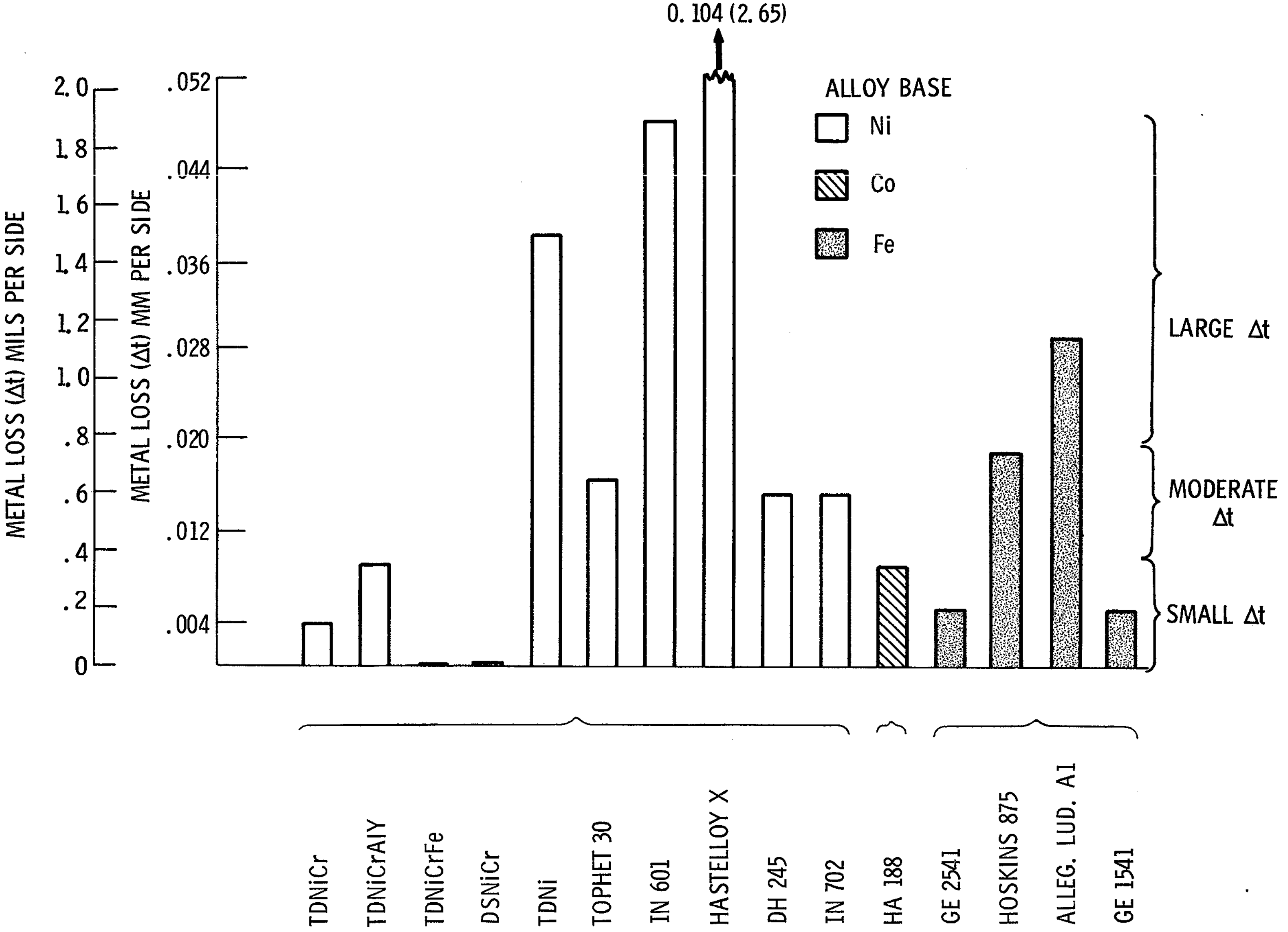

Figure 5. - Metal loss per side for materials cyclically exposed at 1204° C (2200° F), 10 torr air pressure for 50 hours. Test cycle: 30 minutes at 1204° C (2200° F), 6 minute cool.

INITIAL
THICKNESS,
0.49 mm
(19.3 MILS)

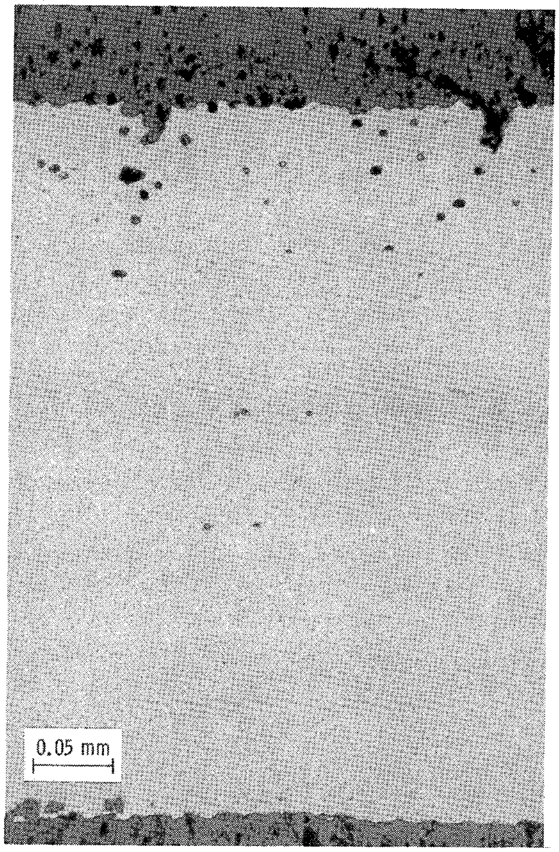

UNETCHED X200

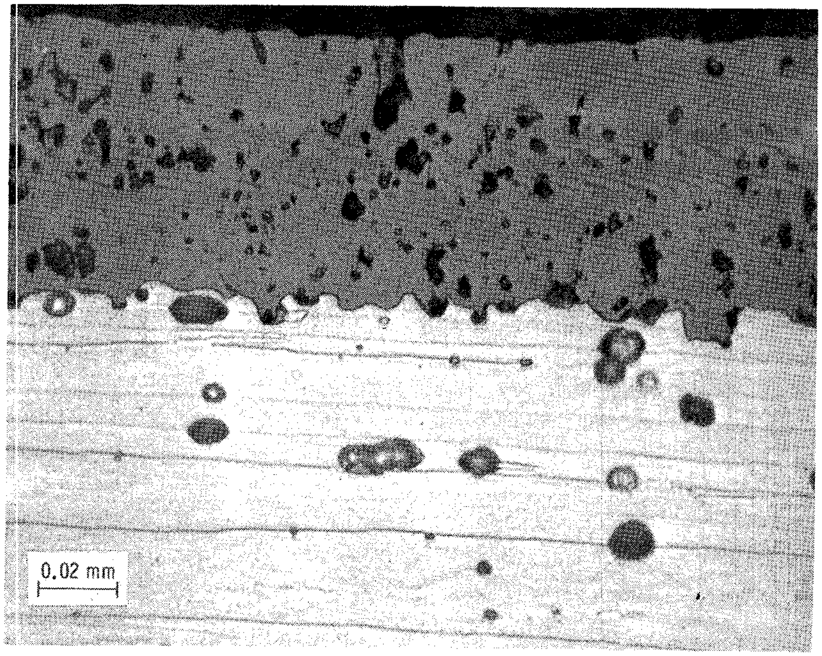

ETCHED X500

Figure 6. - Microstructures of TD Ni exposed at 1204° C (2200° F), 10 torr air pressure for 50 hours (100 cycles). Test cycle: 30 minutes at 1204° C (2200° F), 6 minute cool.

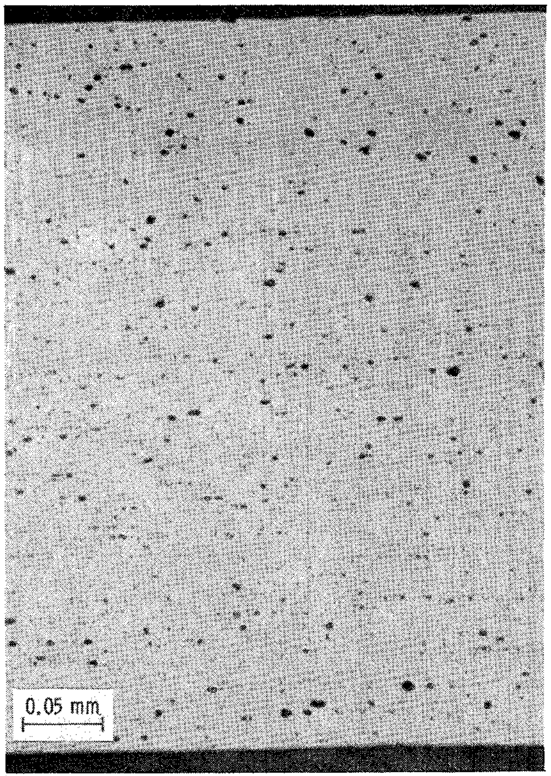

UNETCHED X200

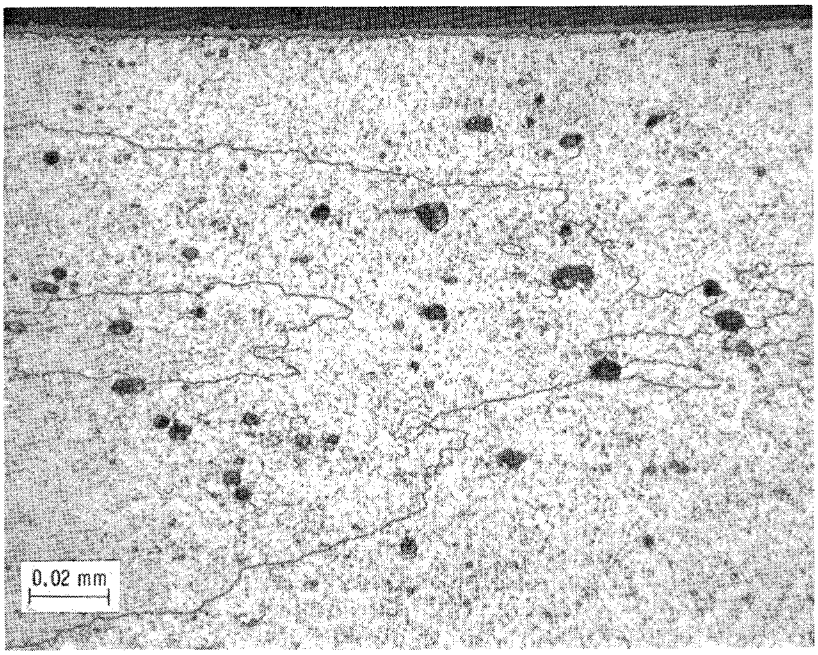

ETCHED X500

Figure 7. - Microstructures of TD NiCr exposed at 1204° C (2200° F), 10 torr air pressure for 50 hours (100 cycles). Test cycle: 30 minutes at 1204° C (2200° F), 6 minute cool.

NOT REPRODUCIBLE

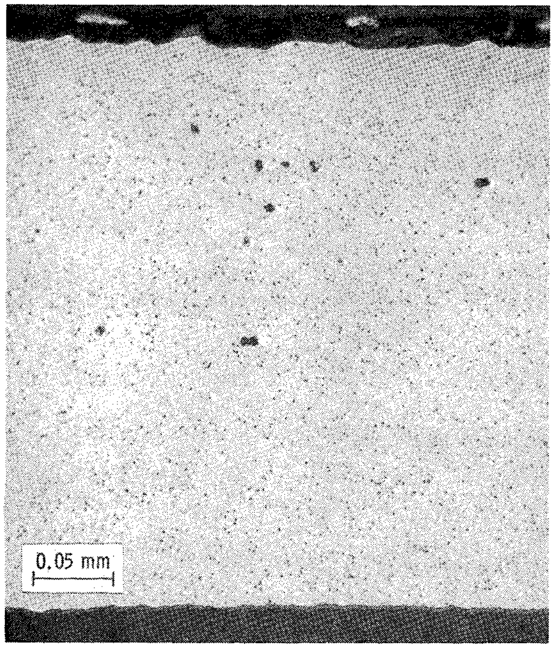

UNETCHED X200

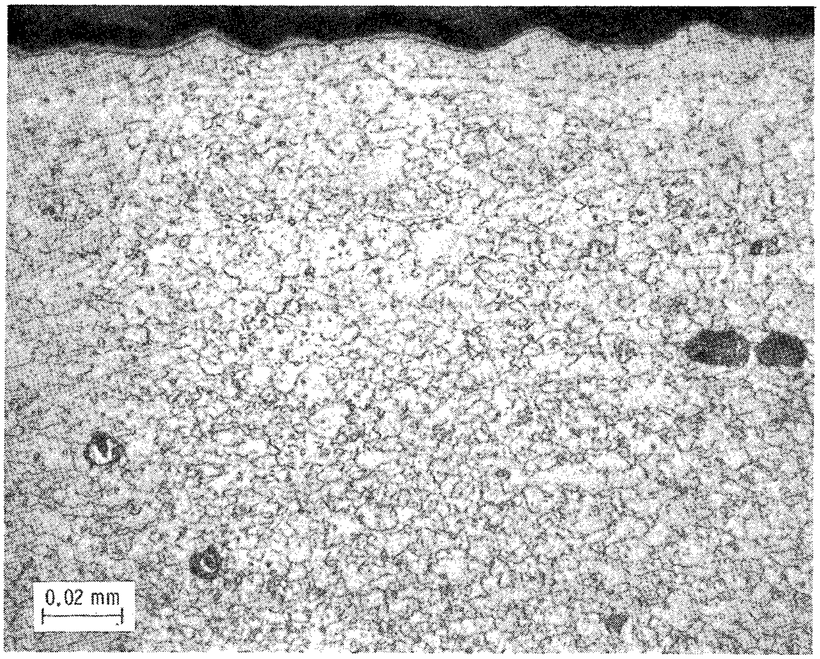

ETCHED X500

Figure 8. - Microstructures of TD NiCrFe exposed at 1204° C (2200° F), 10 torr air pressure for 50 hours (100 cycles). Test cycle: 30 minutes at 1204° C (2200° F), 6 minute cool.

INITIAL THICKNESS, 0.27 mm (10.6 MILS)

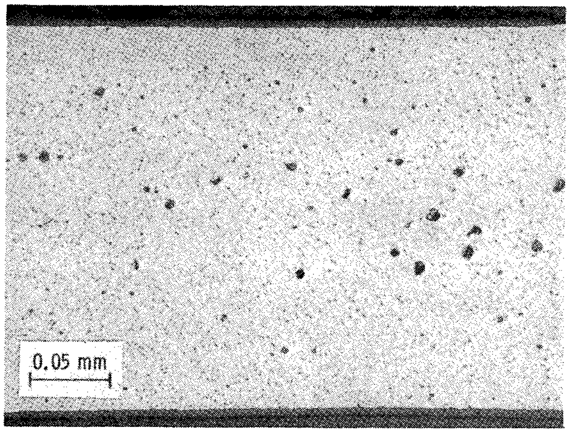

UNETCHED X200

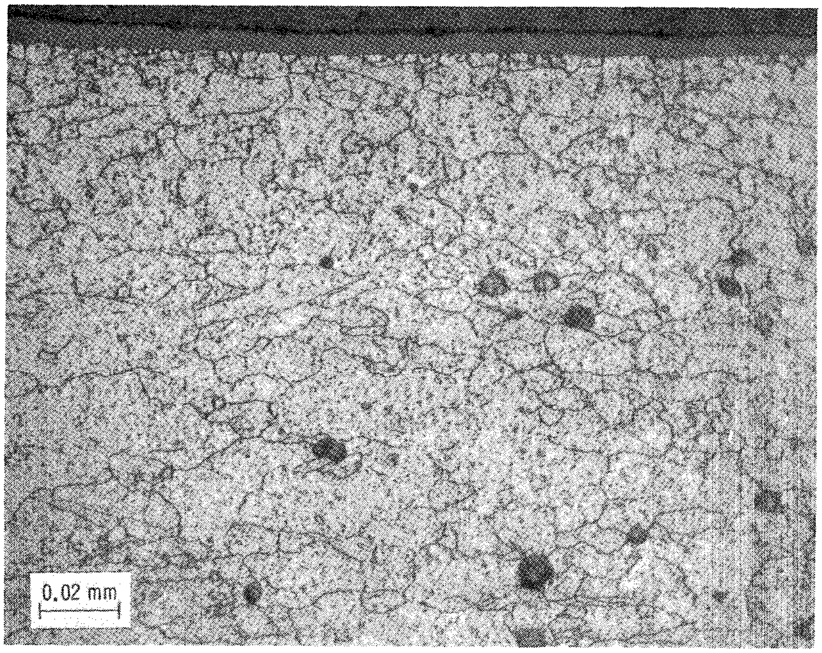

ETCHED X500

Figure 9. - Microstructures of TD NiCrAlY exposed at 1204° C (2200° F), 10 torr air pressure for 50 hours (100 cycles). Test cycle: 30 minutes at 1204° C (2200° F), 6 minute cool.

INITIAL
THICKNESS,
0.29 mm
(11.4 MILS)

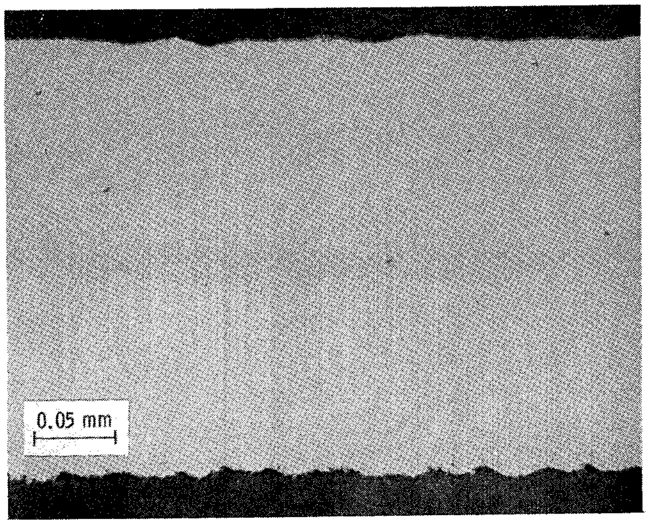

UNETCHED X200

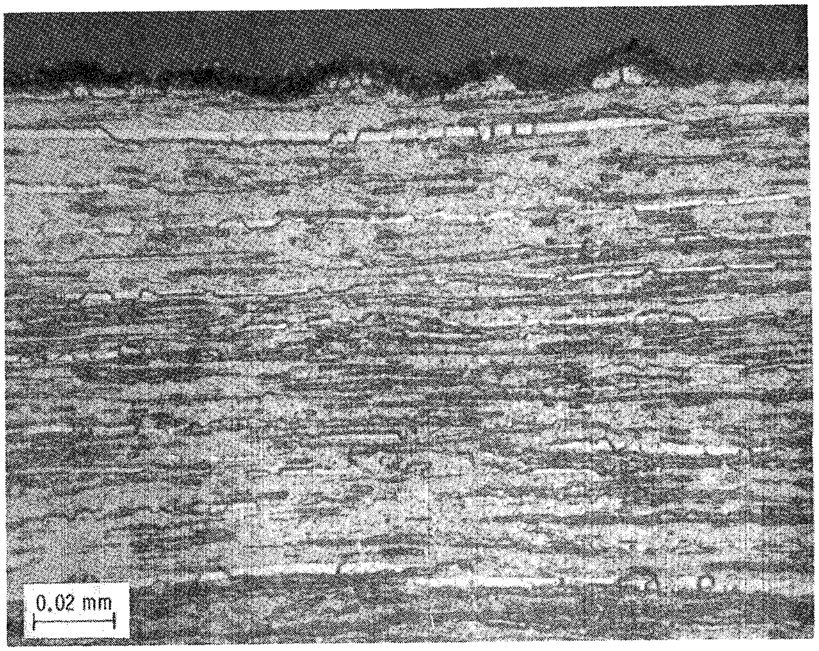

ETCHED X500

Figure 10. - Microstructures of DS NiCr exposed at 1204° C (2200° F), 10 torr air pressure for 50 hours (100 cycles). Test cycle: 30 minutes at 1204° C (2200° F), 6 minute cool.

INITIAL THICKNESS, 0.35 mm (13.8 MILS)

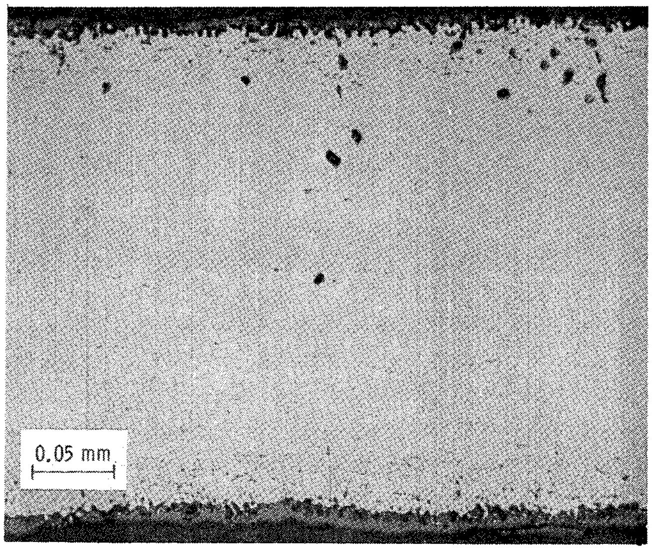

UNETCHED X200

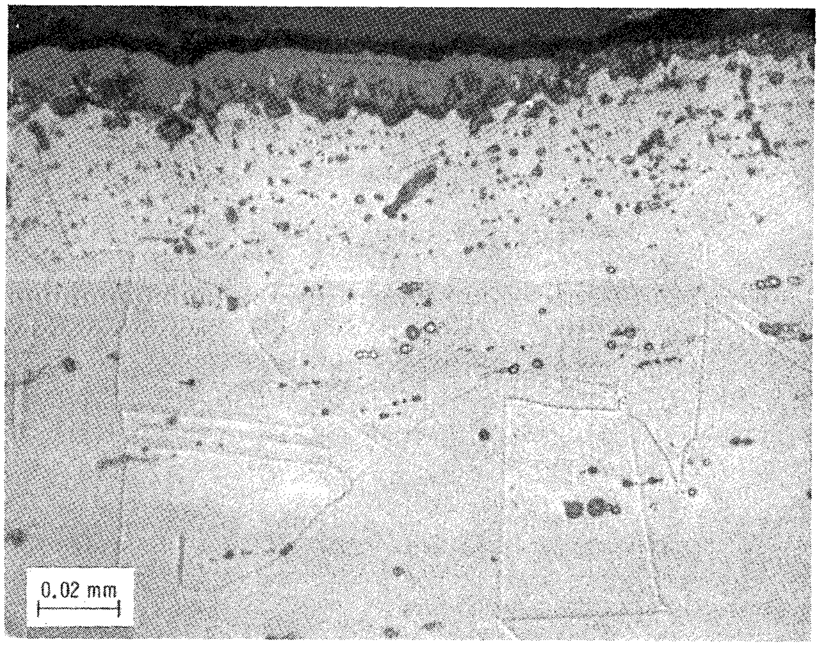

ETCHED X500

Figure 11. - Microstructures of Tophet 30 exposed at 1204° C (2200° F), 10 torr air pressure for 50 hours (100 cycles). Test cycle: 30 minutes at 1204° C (2200° F, 6 minute cool.

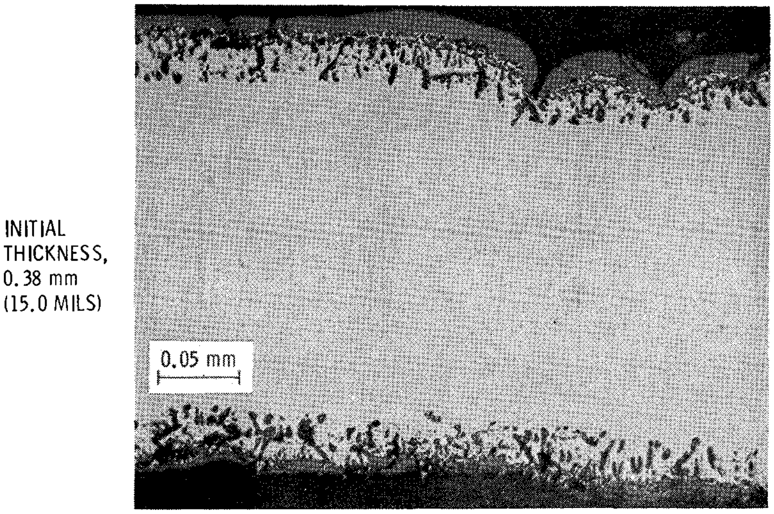

UNETCHED X200

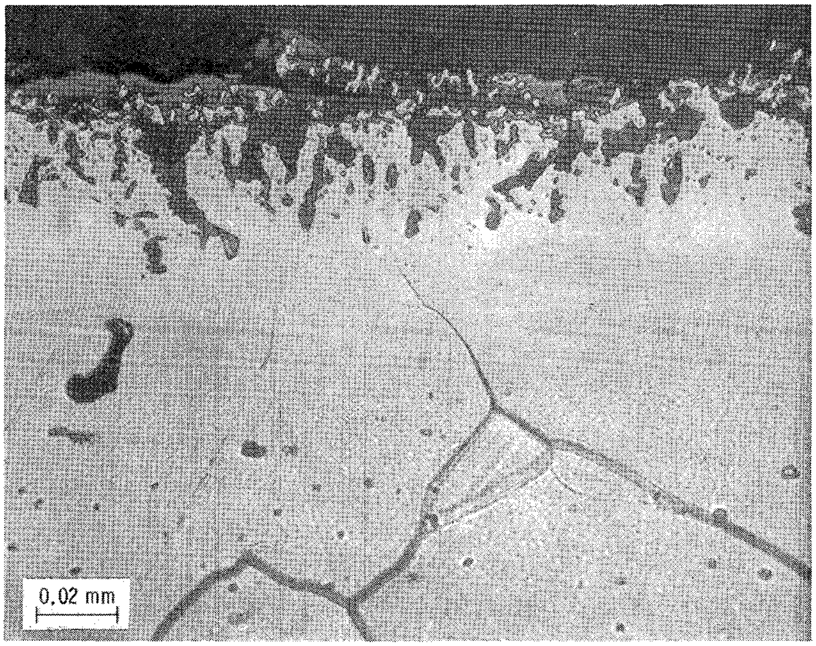

ETCHED X500

Figure 12. - Microstructures of IN 601 exposed at 1204° C (2200° F), 10 torr air pressure for 50 hours (100 cycles). Test cycle: 30 minutes at 1204° C (2200° F), 6 minute cool.

INITIAL
THICKNESS,
0.38 mm
(15.0 MILS)

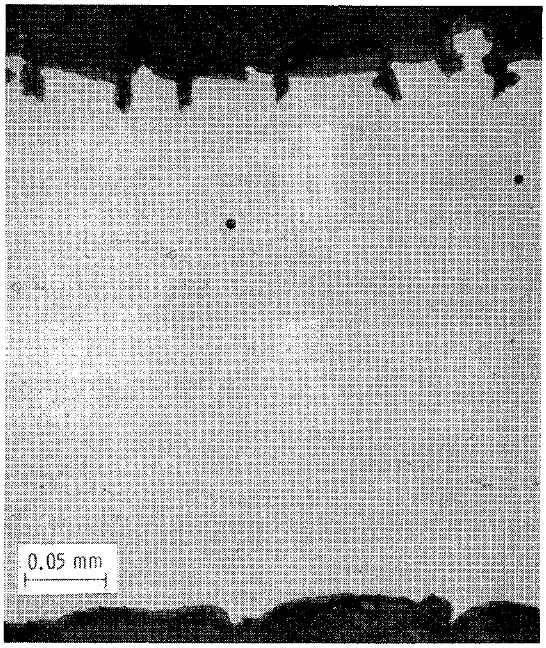

UNETCHED X200

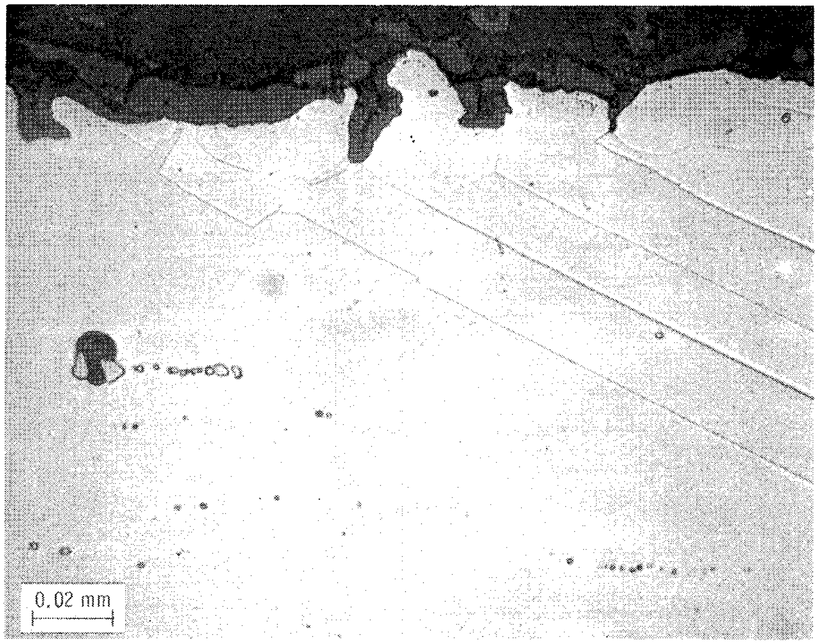

ETCHED X500

Figure 13. - Microstructures of IN 702 exposed at 1204° C (2200° F), 10 torr air pressure for 50 hours (100 cycles). Test cycle: 30 minutes at 1204° C (2200° F), 6 minute cool.

NOT REPRODUCIBLE

INITIAL
THICKNESS,
0.42 mm
(16.5 MILS)

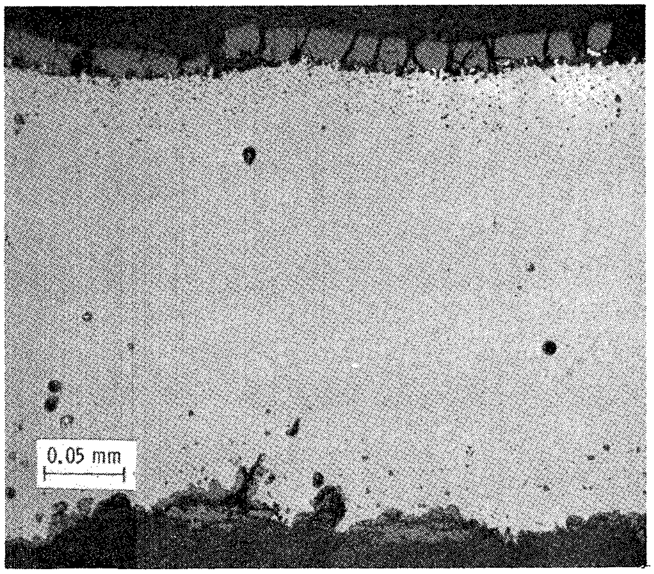

UNETCHED X200

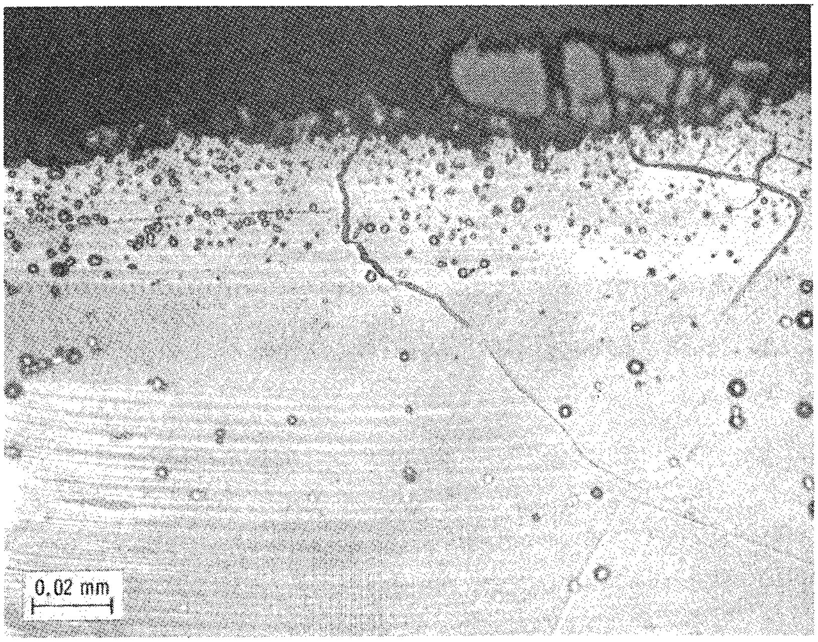

ETCHED X500

Figure 14. - Microstructures of Hastelloy X exposed at 1204° C (2200° F), 10 torr air pressure for 50 hours (100 cycles). Test cycle: 30 minutes at 1204° C (2200° F), 6 minute cool.

INITIAL THICKNESS, 0.41 mm (16.1 MILS)

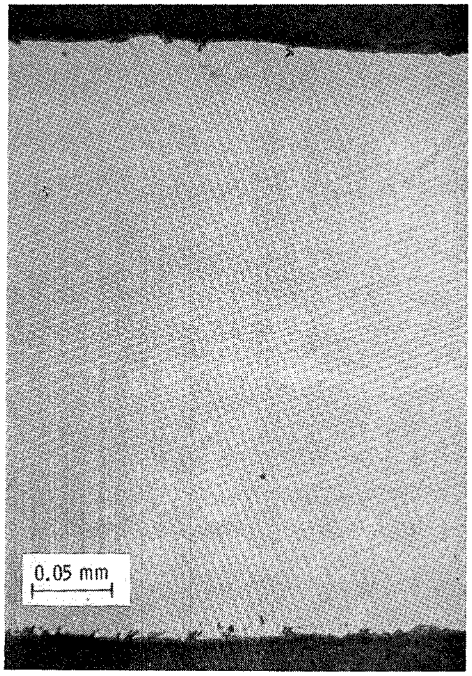

UNETCHED X200

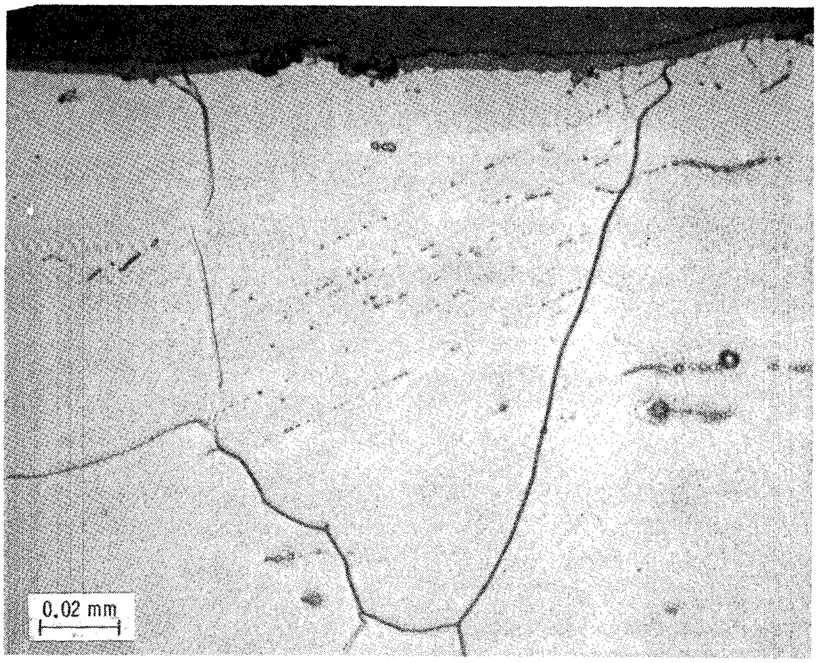

ETCHED X500

Figure 15. - Microstructures of DH 245 exposed at 1204° C (2200° F), 10 torr air pressure for 50 hours (100 cycles). Test cycle: 30 minutes at 1204° C (2200° F), 6 minute cool.

INITIAL
THICKNESS,
0.39 mm
(15.4 MILS)

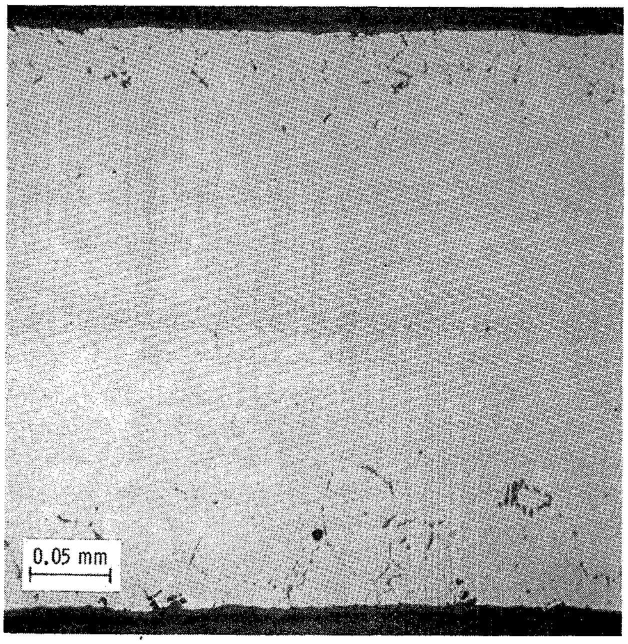

UNETCHED X200

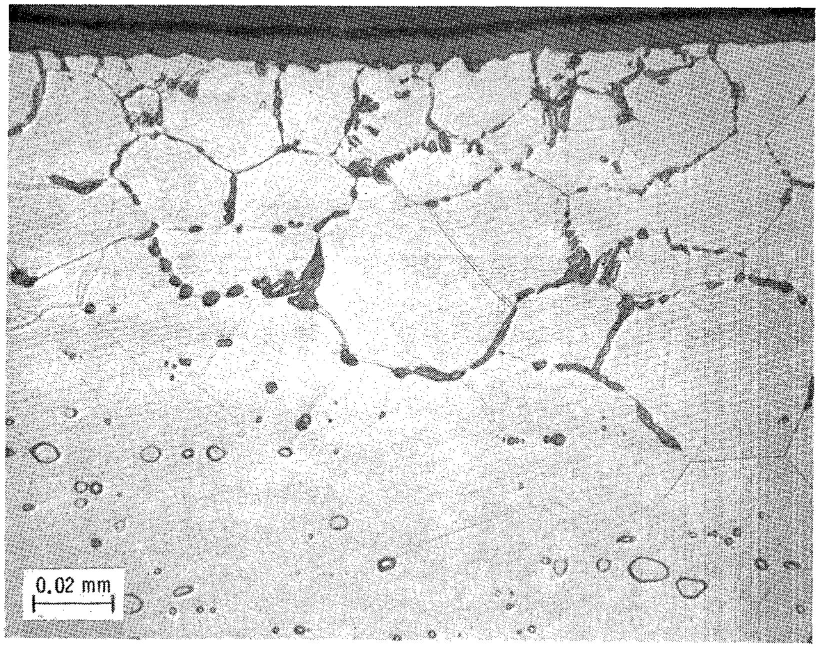

ETCHED X500

Figure 16. - Microstructures of GE 1541 exposed at 1204° C (2200° F), 10 torr air pressure for 50 hours (100 cycles). Test cycle: 30 minutes at 1204° C (2200° F, 6 minute cool.

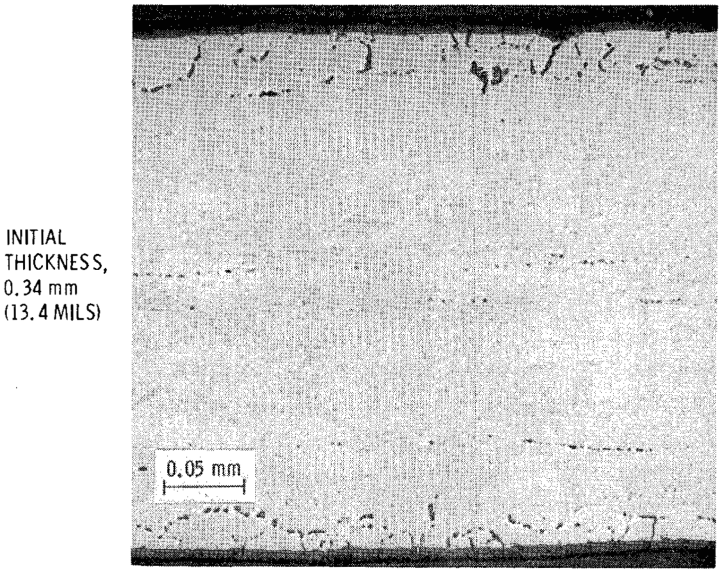

UNETCHED X200

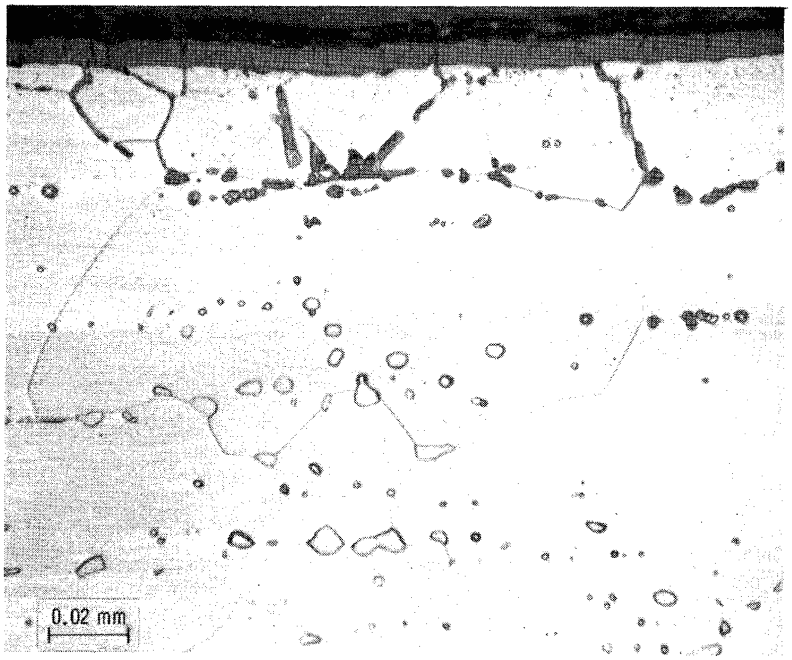

ETCHED X500

Figure 17. - Microstructures of GE 2541 exposed at 1204° C (2200° F), 10 torr air pressure for 50 hours (100 cycles). Test cycle: 30 minutes at 1204° C (2200° F), 6 minute cool.

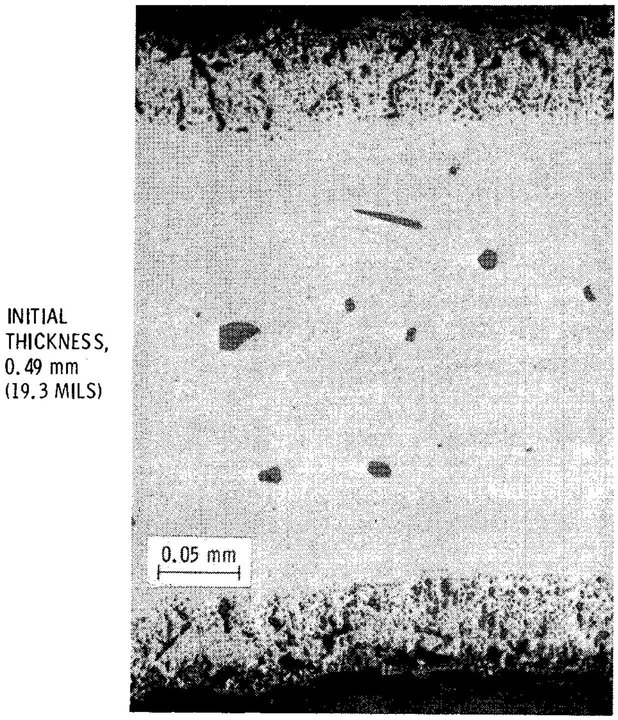

UNETCHED X200

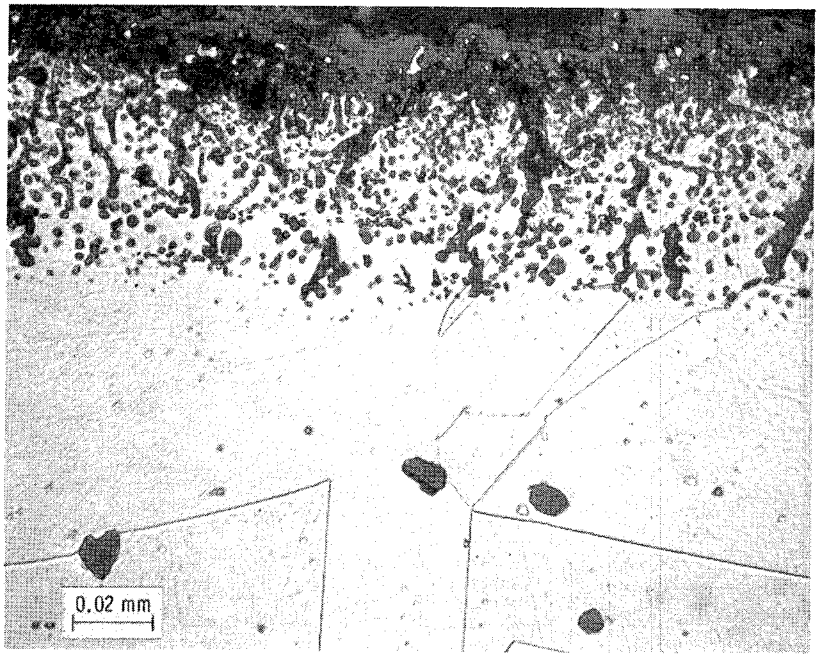

ETCHED X500

Figure 18. - Microstructures of Allegheny Ludlum A1 exposed at 1204° C (2200° F), 10 torr air pressure for 50 hours (100 cycles). Test cycle: 30 minutes at 1204° C (2200° F), 6 minute cool.

INITIAL
THICKNESS,
0.41 mm
(16.1 MILS)

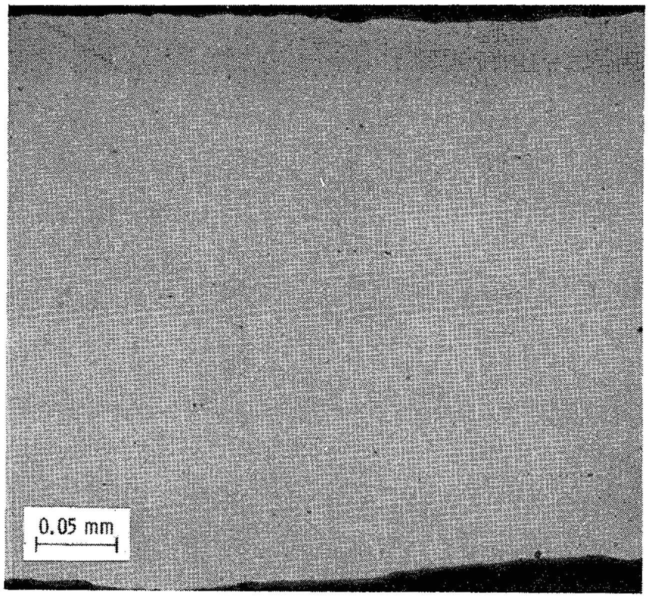

UNETCHED X200

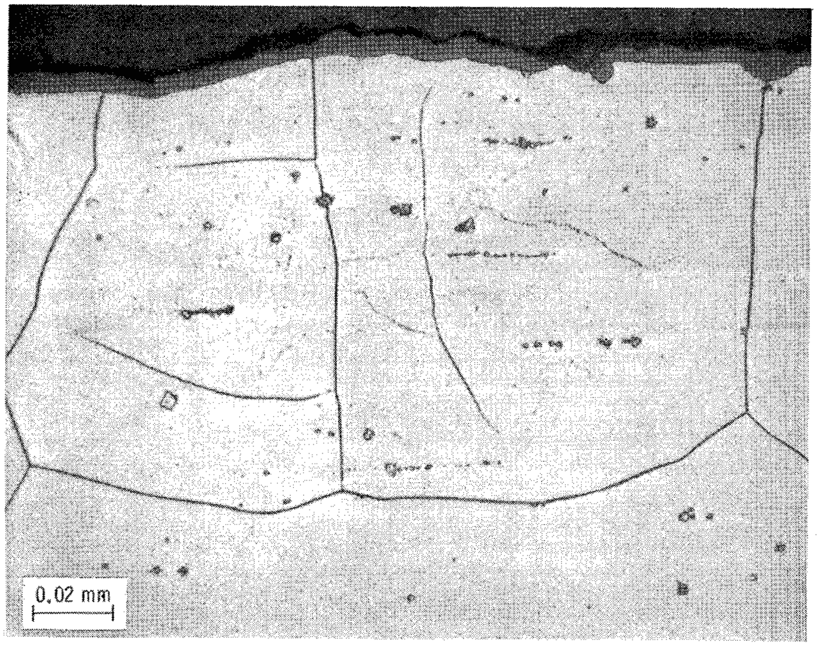

ETCHED X500

Figure 19. - Microstructures of Hoskins 875 exposed at 1204° C (2200° F), 10 torr air pressure for 50 hours (100 cycles). Test cycle: 30 minutes at 1204° C (2200° F), 6 minute cool.

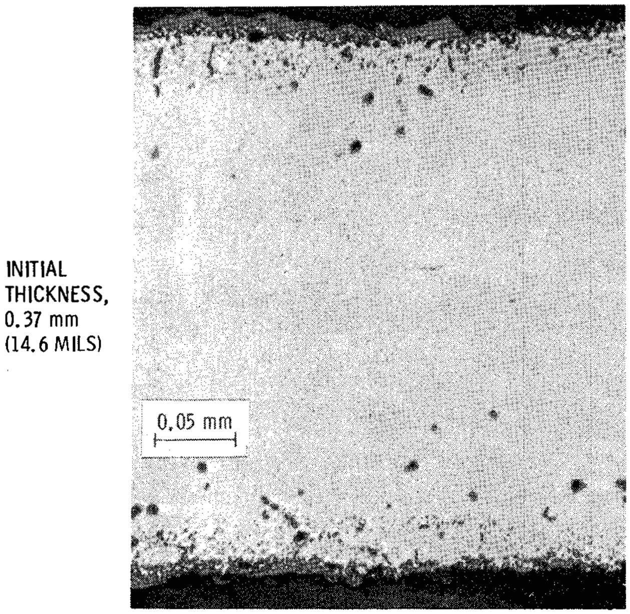

UNETCHED X200

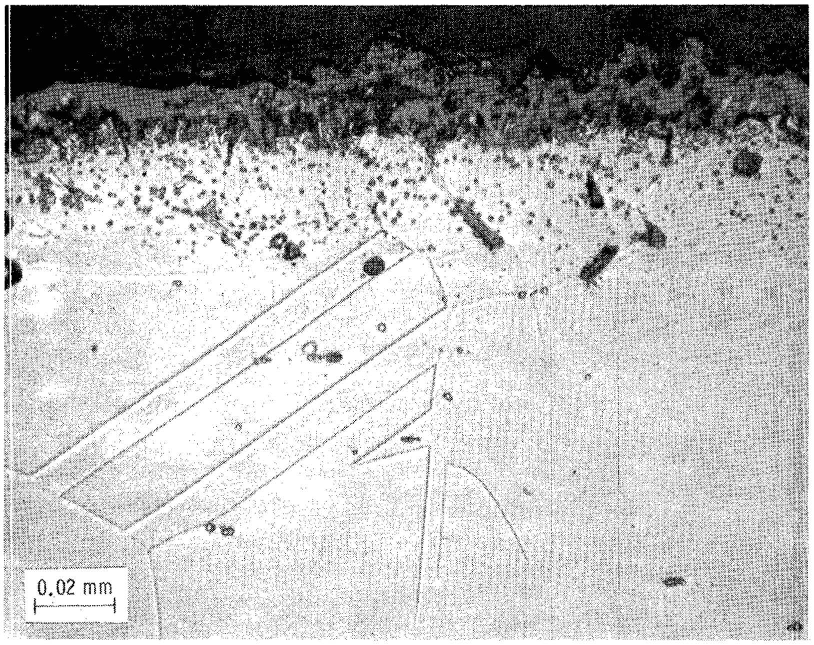

ETCHED X500

Figure 20. - Microstructures of HA 188 exposed at 1204° C (2200° F), 10 torr air pressure for 50 hours (100 cycles). Test cycle: 30 minutes at 1204° C (2200° F), 6 minute cool.